
Towards Efficient Deep Hashing Retrieval: Condensing Your Data via Feature-Embedding Matching

Tao Feng^{1*} Jie Zhang^{1*} Peizheng Wang² Zhijie Wang³
¹Donghua University ¹Zhejiang University

Abstract

The expenses involved in training state-of-the-art deep hashing retrieval models have witnessed an increase due to the adoption of more sophisticated models and large-scale datasets. Dataset Distillation (DD) or Dataset Condensation (DC) focuses on generating smaller synthetic dataset that retains the original information. Nevertheless, existing DD methods face challenges in maintaining a trade-off between accuracy and efficiency. What's more, the state-of-the-art dataset distillation methods can't expand to all deep hashing retrieval methods. In this paper, we propose an efficient condensation framework that addresses these limitations by matching the feature-embedding between synthetic set and real set. Furthermore, we enhance the diversity of features by incorporating the strategies of early-stage augmented models and multi-formation. Extensive experiments provide compelling evidence of the remarkable superiority of our approach, both in terms of performance and efficiency, compared to state-of-the-art baseline methods.

1 Introduction

In recent years, hash algorithms have demonstrated significant effectiveness in retrieving high-dimensional and large-scale data in practical applications owing to their efficient computation and storage capabilities [3, 11, 30, 37]. The existing repertoire of hashing methods includes sensitive local hashing techniques [7, 13, 19, 26] and learning-based hashing approaches. Learning hash functions to obtain effective hashing codes has emerged as a predominant research direction due to the data-independent nature of sensitive local hashing. The utilization of deep learning [27] for obtaining hash codes has garnered significant attention owing to its inherent capacity to generate expressive representations and end-to-end hash codes. Deep hash retrieval exhibits wide-ranging applicability across diverse domains, encompassing image retrieval [12, 16, 32, 50, 55], video retrieval [32, 43, 53], text retrieval [14, 38, 45], and content-based recommendation systems [10, 10, 48].

The primary objective of hash-based image retrieval is to devise an effective approach for representing images using comparable hash codes. Due to the high dimensionality of image features, obtaining compact representations poses a significant challenge. Furthermore, the utilization of large-scale training datasets escalates the computational complexity and training time. In order to address these challenges, we consider the condensation of the training data into a reduced scale to alleviate the computational resource constraints and training duration.

Dataset Distillation (DD) [6, 52], which encompasses the rich information of the original large training set and yields results comparable to the original dataset. In order to minimize the training cost of hash-based image retrieval, it is worth considering the utilization of data distillation techniques to distill the retrieval training set. This enables the retrieval performance trained on synthetic sets achieved on par with that trained on the original dataset. However, in light of the fundamental objective of deep hash retrieval, which seeks to ascertain a hash function imbued with desirable mapping characteristics,

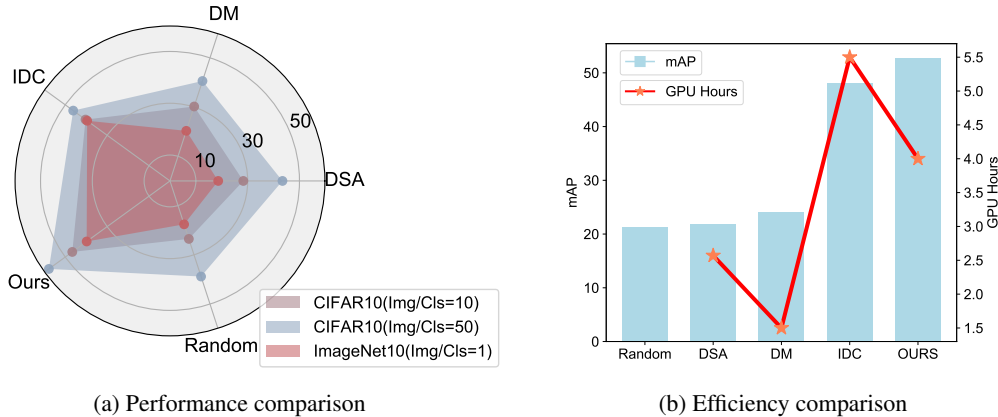


Figure 1: The performance and efficiency comparison between our method and the state-of-art baselines. The performance analysis on CIFAR10 (10/50 images per class) and ImageNet10 (1 image per class) is visually represented in Figure (a), with the colors pale violet red, red, and turquoise corresponding to the respective datasets. Figure (b) presents a graphical depiction of the mean Average Precision (mAP) achieved by various dataset distillation methods on ImageNet10 (3 images per class), displayed as a blue bar graph, and the corresponding GPU hours required to achieve convergence, represented by the red plot.

the loss of a considerable amount of critical features during dataset distillation exerts a momentous influence on the precision of retrieval. Furthermore, when considering the extensive utilization of deep hashing retrieval in the realm of large-scale datasets, the current DD methodologies [6, 21, 23, 58, 59] do not adequately reconcile the exigencies of accuracy and efficiency in distilling vast data ensembles, thus incurring significant distillation costs.

As illustrated in Figure 1a, utilizing the currently preferred distillation method [23, 58, 59] to distill dataset for image hashing does not yield significant improvements compared to random selection of the requisite number of images from each category. This undermines the purpose of acquiring condensed data. Consequently, it is imperative to choose an appropriate distillation technique in order to obtain superior condensed data that facilitates the generation of compact hash codes conducive to deep hashing retrieval.

In this study, with the primary objective of synthesizing data without sacrificing pivotal features for hashing codes and reducing training cost of DD, we propose a distillation approach grounded in feature-embedding matching [59]. Additionally, due to the limited availability of features in the synthetic feature space, we delve into the investigation of Early-Stage augmented Models [57] and multi-formation techniques [23], aiming to bolster the diversification of early feature information for improved capture of informative features. Figure 1b elucidates the substantial efficacy of our proposed approach in comparison to IDC [23], showcasing an impressive performance gain of around 4% and 1× speed up on ImageNet10 with 3 images per class.

Our main contributions can be concluded as:

- To the best of our knowledge, this investigation stands as the inaugural work in the realm of distilling datasets applied for deep hashing retrieval, leading to enhanced training speed and reduced training cost in the context of image hashing techniques.
- Leveraging the synergistic impact of Early-Stage augmented Models and multi-formation approaches, we effectively align the feature-embedding process, thereby facilitating the efficient capture of diverse features from the real dataset.
- The experimental findings unequivocally establish the supremacy of our proposed method over previous DD methodologies [23, 58, 59], demonstrating not only enhanced effectiveness but also remarkable improvements in distillation efficiency.

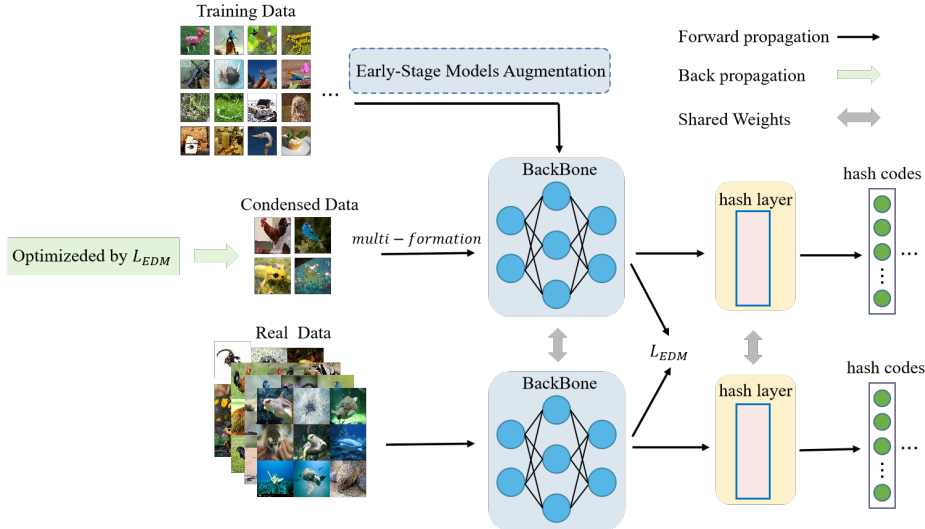


Figure 2: The illustration of our proposed method (IEM) for deep hashing retrieval.

2 Method

2.1 Overview

To enhance the performance of distillation datasets in the context of retrieval tasks, we propose an effective technique called Information-intensive Feature-Embedding Matching (IEM). The schematic representation of our proposed IEM framework is presented in Figure 2. Our approach involves the selection of weight-perturbation pre-trained networks during the initial phase, encompassing a wide range of information within the feature space. Subsequently, the condensed dataset is optimized via feature-embedding matching [59], utilizing the pools of networks from the early stages [57]. We show detailed Related Work and Preliminary in the **Appendix**.

2.2 Speed and Generalization: Feature-Embedding Matching

Existing DD methods [2, 9, 21, 35, 36, 47], especially gradient-matching method [23, 58, 60], has demonstrated remarkable effectiveness in classification tasks [25]. This can be attributed to the simplicity of employing a single cross-entropy loss, which enables seamless gradient-matching. However, when it comes to image hashing, the objective shifts to generating discriminative binary codes while simultaneously minimizing quantization errors. Consequently, multiple optimization objectives need to be considered. For instance, methods like DHD [20] require optimizing hash layer parameters using Self-distilled Hashing loss, proxy-based representation loss, and Binary Cross Entropy-based (BCE) quantization loss. Similarly, CSQ [56] employs Central Similarity Quantization loss and quantization loss. As a result, various image hashing methods necessitate distinct gradient-matching approaches tailored to their specific optimization objectives, resulting in a complex gradient-matching process. Additionally, gradient-matching typically entails computationally expensive bi-level optimization, leading to prolonged training times.

The main objective of distribution-matching method [51, 59] is to generate synthetic datasets that accurately capture the distribution of real datasets in the feature space. which involves embedding each real image $x \in \mathbb{R}^d$ into a lower-dimensional space, preserving essential information from the original input. Notably, the utilization of hash codes generated by image hashing enables efficient storage and content representation of input images. Consequently, for effective deep hashing retrieval, synthetic data should exhibit informative representations in the feature space that are on par with real datasets. Building on this inspiration, we focus on minimizing the discrepancy between the embedding-feature distributions of synthetic and real datasets, which is critical for generating information-intensive hash codes. Furthermore, embedding matching offers the advantage of circumventing the expensive training costs associated with alternative methods [23, 58], and facilitates easy integration with existing deep hashing approaches [4, 5, 16, 20, 54, 61].

2.3 Information Strengthen in Feature Space

The distribution-matching method aims to embed synthetic data into feature space that effectively interprets its inputs. This necessitates matching in a diverse and informative feature space. However, existing methods [51, 59] generally match features obtained from randomly initialized networks, which may not capture the typical feature distribution. Inspired by the Model Augmentation [57] method, we propose selecting early-stage augmented networks to enrich the diversity of the feature space, thereby providing ample potential for feature-embedding matching. Furthermore, traditional distribution-matching methods directly optimize each data element, such as pixel by pixel, without imposing any regularity conditions on the synthetic data. This limitation restricts the information content in the feature space. Therefore, we adopt a multi-formation [23] method to enhance the effectiveness of feature distribution.

2.4 Training Algorithm

Our methodology is outlined in Algorithm 1. Departing from the customary practice of initializing networks randomly prior to dataset condensation, we employ an early-stage network augmentation method [57]. We conduct a comprehensive training of condensed data involving R outer loops and M inner loops. Within each outer loop, we select a network from a pre-arranged pool of early-stage enhanced networks. Throughout each inner loop, the condensed dataset is optimized through the minimization of the feature-embedding discrepancy between the intra-class mini-batches T_c and S_c , respectively. Notably, the number of outer loops is adjusted based on the specific dataset. For low-resolution images, we set R to 300, while for high-resolution images, R is set to 200.

Algorithm 1: Dataset Condensation for Hashing Retrieval

Input: Training set \mathcal{T}
Output: Synthetic set S

- 1 **Notation:** Multi-formation function f , parameterized augmentation function a_w , loss function l , number of classes N_c , deep neural network ψ_θ , deep hashing neural network Φ_θ parameterized with θ .
- 2 **for** $q \leftarrow 0$ **to** Q **do**
- 3 | Update networks w.r.t. hashing retrieval losses
- 4 **end**
- 5 Initialize condensed dataset S
- 6 **for** $r \leftarrow 0$ **to** R **do**
- 7 | Randomly load one checkpoint from pre-trained Φ_θ ;
- 8 | **for** $m \leftarrow 0$ **to** M **do**
- 9 | | **for** $c \leftarrow 0$ **to** N_c **do**
- 10 | | | Sample an intra-class mini-batch $T_c \sim \mathcal{T}, S_c \sim S$
- 11 | | | $L = \left\| \frac{1}{|T_c^T|} \sum_{(x,y) \in T_c^T} \psi_\theta(a_w(f(x))) - \frac{1}{|S_c^T|} \sum_{(s,y) \in T_c^T} \psi_\theta(a_w(f(x))) \right\|^2$
- 12 | | | Update $S_c \leftarrow S_c - \eta \nabla_c(L)$
- 13 | | **end**
- 14 | **end**
- 15 **end**

3 Experiments

3.1 Datasets and Implementation Details

Datasets. In this study, we employed widely utilized datasets [20, 31] for retrieval purposes, including CIFAR10 [24], ImageNet [39]. The details of these datasets are provided in **Appendix**.

Network Architectures. Conforming to the settings in the previous distillation methodologies [23, 59], we employed ConvNet-3 [40] for the low-resolution dataset CIFAR10, and ResNetAP-10 [15] for the high-resolution datasets ImageNet.

Evaluation Metrics. To assess the performance of distilled datasets in retrieval tasks [12, 16, 20], we adopt the same approaches employed in prior distillation approaches [23, 58, 59]. We train a deep

hashing network using distilled data and subsequently test its performance on the query set in retrieval. The evaluation metrics used in previous deep hashing tasks [16, 20, 46] are adopted, including mean average precision (mAP) and precision with respect to top-M returned image (P@Top-M) [8]. We employed hash code lengths of 32 and 64 bits and evaluated their effectiveness on two separate code scales. The top-M values for calculating mAP varies across the datasets [20]: CIFAR10@5000, ImageNet10@1000, and ImageNet20@1000.

3.2 Condensed Dataset Evaluation.

Baselines. To the best of our knowledge, this research paper represents the first comprehensive investigation of dataset distillation for deep hashing retrieval. In order to condense the datasets, we employ an array of condensation methodologies as our baseline, including (1) gradient matching methods: DSA [58] and IDC [23], and (2) distribution matching method : DM [59]. As for the deep hashing retrieval process, we utilize the state-of-the-art method DHD [20] as our image hashing benchmark. To further substantiate the generalizability of our method , we extend its application to a diverse set of deep hashing retrieval approaches, such as DPN [12], and OrthoHash [16]. We show detailed Experimental Settings in the **Appendix**.

Img(s)/cls	Ratio	Bites	Random	DM	DSA	IDC	IEM	Whole set
1	0.2%	32	14.83	18.46	15.12	23.67	24.21	68.15
		64	15.35	18.62	15.73	24.65	25.82	70.21
10	2%	32	22.99	29.95	27.23	38.92	45.32	68.15
		64	23.54	30.23	28.32	40.32	45.85	70.21
50	10%	32	35.47	41.12	39.83	46.78	55.72	68.15
		64	38.82	43.43	40.58	46.21	57.49	70.21

Table 1: Comparing to different training set synthesis methods for deep hashing retrieval on CIFAR10. We first generate synthetic data using these methods and subsequently assess their effectiveness by training neural networks from scratch. The terms Img(s)/cls and Ratio (%) denote the number of image(s) per class and the condensed set size as a percentage of the entire training set size, respectively.

CIFAR10. The training set utilized for image hashing retrieval in CIFAR10 consists of 500 images per class with resolution of 32×32. To more clearly illustrate the effect of dataset condensation, we distill CIFAR10 to 1/10/50 images per class like previous works [23, 58, 59]. We evaluate the effectiveness of ConvNet-3 on each synthetic set(s) based on mean average precision (mAP) for 32 and 64 bits of hash codes, with the results presented in Table 1. The experimental results demonstrate that IDC [23] achieves significant improvements over DSA [58] and DM [59], owing to its utilization of the multi-formation process that defines an enlarged and regularized data space for optimizing synthetic sets. Notably, our proposed method surpasses IDC [23] by approximately 6% and 12% at 10 and 50 images per class respectively. However, our method achieves comparable performance on 1 image per class. One possible factor contributing to this observation is the limited information being mapped into the feature space on smaller synthetic data.

To further investigate the improved retrieval quality of the condensed datasets generated by our method compared with the state-of-the-art IDC [23], we present the mean average precision (mAP) scores across different epoch steps and the P@Top-M curves (widely used in retrieval tasks) at 64 bits of hash codes. As depicted in Figure 3a and Figure 3b, our method consistently outperforms the baseline methods in terms of mAP scores at each epoch, demonstrating the effectiveness of our feature-embedding alignment approach in generating more informative synthetic datasets. Moreover, as shown in Figure 4 and Figure 5, the condensed dataset produced by our method simultaneously achieves higher precision at lower recall levels, further indicating the capacity and utility of our approach in distilling better training sets for retrieval tasks.

ImageNet. High-resolution datasets are commonly employed in retrieval tasks, thus motivating us to investigate the effectiveness of our proposed method for distilling ImageNet10/20. Unlike prior work, we distill ImageNet-subset to 1/3 images per class, with each class containing 1200 images. It is noteworthy that we intentionally avoid employing the pre-trained network trained on the entirety of the ImageNet. This choice is aimed at ensuring a just assessment of the effects for distillation methods. Table 2 presents the mean average precision (mAP) of ResNetAP-10 trained on

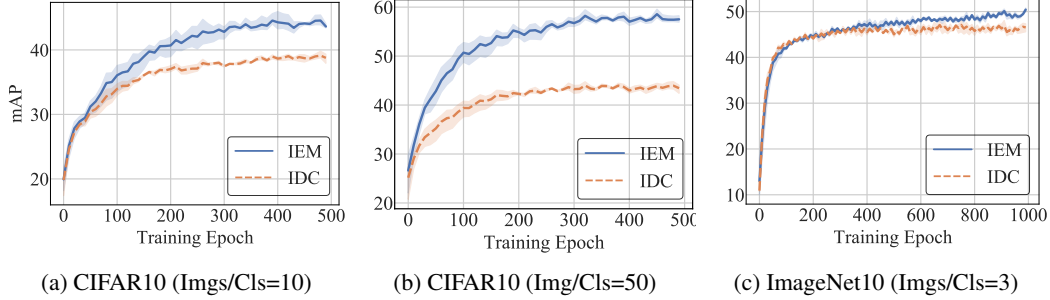


Figure 3: mAP curves on CIFAR10 and ImageNet10 across various training epochs with binary codes @ 64-bits. The term Imgs/cls denotes the number of images per class.

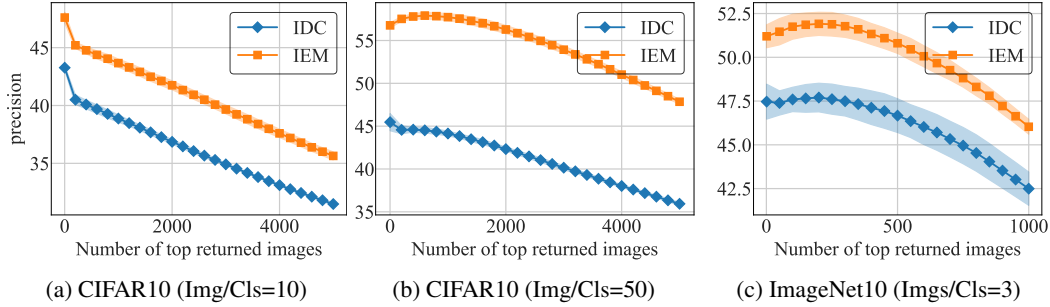


Figure 4: Precision@top-5000 curves on CIFAR10 and Precision@top-1000 curves on ImageNet10 with binary codes @ 64-bits. The term Imgs/cls denotes the number of images per class.

each synthetic set(s) for 32 and 64 bits of hash codes. As illustrated in Table 2, both DM [59] and DSA [58] exhibit comparable performance when compared to Random selection on the ImageNet-subset, which demonstrates that these methods fail to adapt effectively to distill high-resolution datasets for deep hashing retrieval. It is noteworthy that our proposed method demonstrates superior performance across different numbers of classes and condensation ratios, outperforming most of the baseline techniques. Figure 4c and Figure 5c show desirable retrieval results of our method compared with ImageNet10. Interestingly, when considering the overall performance, IDC [23] achieves comparable results, particularly surpassing our method on ImageNet20. Nonetheless, it is important to acknowledge that the benefits of IDC [23] come at the expense of its own costly distillation process. In contrast, our method achieves approximately 5 times faster speeds at each compression step and converges more rapidly compared to IDC [23]. A comprehensive analysis is presented in the efficiency comparison section. Additional results are available in the **Appendix**.

Cross-Architecture Generalization. To assess the generalization capacity of our condensed datasets, we conduct experiments using more sophisticated architectures in comparison to ConvNet-3 and ResNetAP-10 trained on condensed datasets of CIFAR10 (50 images/class) and ImageNet10 (3 images/class) respectively. We set the binary code length to 64 and present the results in Table 3.

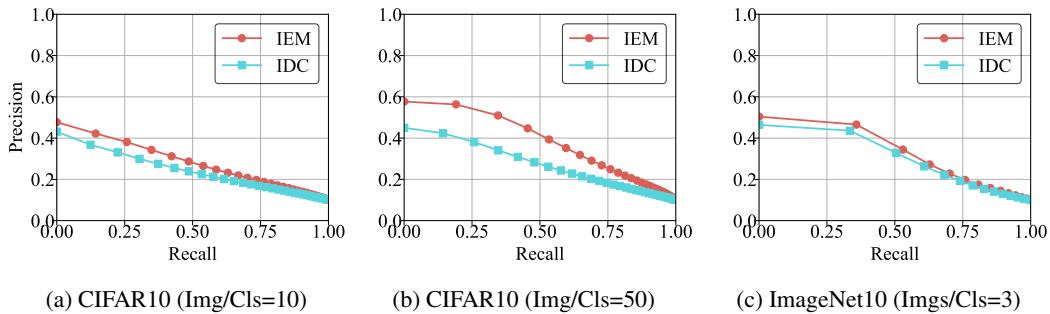


Figure 5: Precision-Recall curves on CIFAR10 and ImageNet10 with binary codes @ 64-bits. The term Imgs/cls denotes the number of images per class.

	Img(s)/cls	Ratio	Bites	Random	DM	DSA	IDC	IEM	Whole Set
ImageNet10	1	0.77%	32	16.46	19.84	18.63	37.21	38.32	63.87
			64	17.62	20.43	18.42	39.55	40.32	66.05
	3	2.3%	32	20.48	21.95	20.93	45.78	48.69	63.87
			64	21.22	24.10	21.78	48.14	52.79	66.05
ImageNet20	1	0.77%	32	10.47	10.22	10.94	24.89	24.23	52.05
			64	10.14	11.22	10.84	26.60	25.70	57.18
	3	2.3%	32	10.88	12.88	11.73	32.89	33.34	52.05
			64	10.71	12.96	11.78	34.48	35.12	57.18

Table 2: Comparing to different training set synthesis methods on deep hashing retrieval on ImageNet-subset. The terms Img(s)/cls and Ratio (%) denote the number of image(s) per class and the condensed set size as a percentage of the entire training set size, respectively. The methods all employ ResNetAP-10.

Dataset	Bites	Methods	Evaluation Models		
			ConvNet-3	ResNet-10	DenseNet-121
CIFAR10	64	IDC	47.14	39.29	35.93
		IEM	59.12	53.42	49.76

(a) The performance of condensed CIFAR-10 dataset (50 images per class).

Dataset	Bites	Methods	Evaluation Models		
			ResNetAP-10	ResNet-18	ResNet-50
ImageNet10	64	IDC	46.08	44.33	41.87
		IEM	52.79	53.53	52.61

(b) The performance of condensed ImageNet10 dataset (3 images per class).

Table 3: Cross-architecture retrieving performance (%) on CIFAR10 and ImageNet10 . The networks are trained on condensed dataset and evaluated on query dataset.

Specifically, we evaluate the ResNet-10 [15] and DenseNet-121 [18] architectures on CIFAR10 and ResNet-18 [15] and ResNet-50 [15] on ImageNet10 as contrastive architectures.

The results presented in Table 3a demonstrate that our proposed method outperforms IDC [23] in terms of generalization performance. For instance, our method surpasses IDC [23] by 2% and 1% on CIFAR10 when evaluated with ResNet-10 [15] and DenseNet-121 [18], respectively. Similarly, as in Table 3b our method outperforms IDC [23] by 9% and 11% on ImageNet10 when evaluated with ResNet-18 [15] and ResNet-50 [15], respectively. An interesting observation is that, in contrast to prior studies [23, 42, 57, 59] that report a decrease in cross-architecture accuracy, our proposed method achieves better and similar performance when tested with ResNet-18 [15] and ResNet-50 [15] compared to using the distilled architecture of ResNetAP-10. This finding highlights the strong generalization ability of the synthetic data distilled by ResNetAP-10 using our approach, which can adapt to sophisticated architectures with deeper depth. Given the simpler architecture of ConvNet-3 in comparison to the ResNet [15] and DenseNet [18] series, it is reasonable to expect that the synthetic data evaluated on more complex and sophisticated architectures may exhibit some deviations, thereby resulting in a reduction.

Efficiency Comparison. Previous research [23, 57] has demonstrated the effectiveness of gradient matching methods in achieving high accuracy, although this is achieved at a considerable cost, due to the complexity of the bi-level optimization and the computation of second-order derivatives. This results in a low distillation efficiency, which can hinder the practical applications of such methods. In this study, we aim to address this issue by proposing a method that achieves high accuracy while maintaining efficiency. Specifically, we evaluate the performance and efficiency between IDC [23] and our method in Figure 6, which are evaluated using the same GPU as the corresponding methods. Additionally, we evaluate the training time for distilling CIFAR-10 and ImageNet-subset, using RTX-2080 Ti and RTX 3090, respectively. As depicted in Figure 6a and Figure 6b, our novel approach demonstrates superior performance in terms of distillation time, surpassing the traditional IDC [23] methodology on CIFAR10. Figure 6d and Figure 6e illustrate that our method achieves a level of precision comparable to IDC [23] on ImageNet10 and ImageNet20. However, the noteworthy aspect of our method lies in its rapid convergence. The visual representation in the Figure 6c and Figure 6f

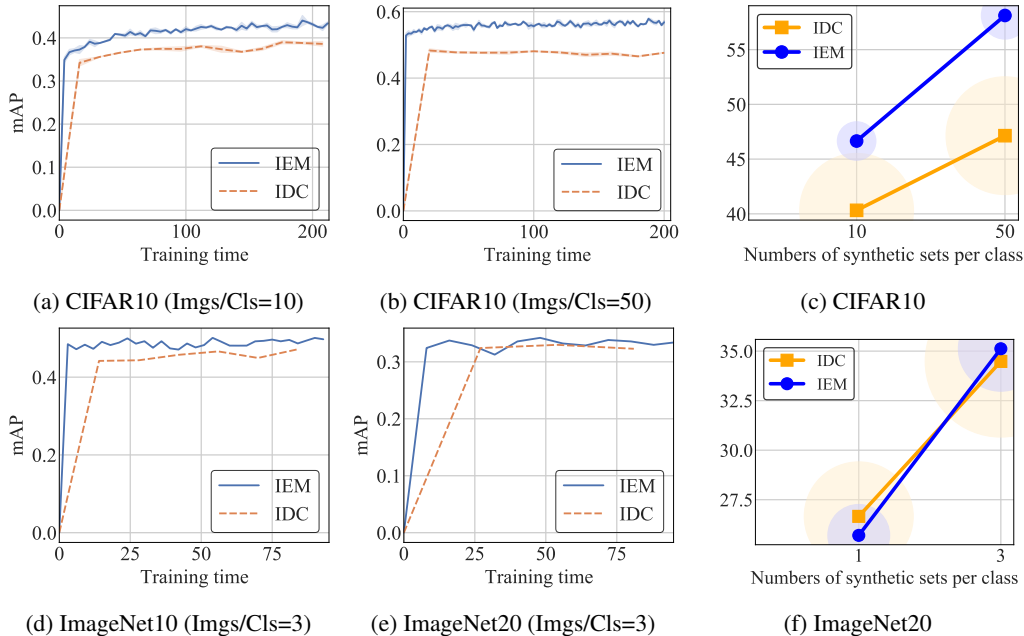


Figure 6: Performance comparison across DD time of IEM and IDC [23]. The utilization of blue and green circles in Figure 6c and Figure 6f signifies the temporal requirements for achieving convergence in IEM and IDC [23], respectively. The dimensions of the circles represent the corresponding time duration needed for convergence in each method.

clearly indicates that our method surpasses IDC [23] or attains comparable results while requiring a lower training cost. These observations highlight the potential of matching feature embedding for effective information extraction. In contrast, gradient matching method in IDC [23] may suffer from biases due to the diversity and complexity of gradient-wise, resulting in compromised matching accuracy and low speed. Specifically, condensing large scale datasets using IDC [23] can incur considerable computational costs (e.g., taking 500 hours for condensing ImageNet10 on RTX 3090), while our method achieves better results in a shorter time. Our findings highlight the potential of our method for practical data condensation and retrieval applications.

Ablation Study on Network Distribution.

To investigate the impact of two strategies in our methods, we conducted ablation experiments on Early-Stage augmented Models [57] and multi-formation [23] in IEM. Comparative analysis is performed between CIFAR-10, with each class distilled to 10/50 images, and ImageNet-10, with each class distilled to 10 images. The results presented in Table 4 demonstrate that IEM’s performance is significantly compromised when distilling without the incorporation of these two components. Specifically, when using Early-Stage augmented Models individually, the performance of IEM drops to 47.00% and 30.23%. In contrast, when using multi-formation individually, the performance improves significantly to 57.73% and 47.63%, approaching the performance achieved by our methods. These findings indicate that Early-Stage augmented Models primarily focus on enhancing diversity within the original feature space, while multi-formation provides more comprehensive and informative representations within the feature space.

	Imgs/Cls	ESP	MF	Performance
CIFAR10	50	✗	✗	43.22
		✓		47.99
		✓	✓	57.88
ImageNet10	3	✗	✗	25.83
		✓		30.23
		✓	✓	50.38

Table 4: Evaluation of the two components in IEM. We present the performance of synthetic data (50 images per class and 3 images per class) of CIFAR10 and ImageNet10. ESP and MF represent strategies of early-stage augmented models and multi-formation.

Generalization on Synthetic Data Cross Deep Hashing Methods. To evaluate the generalization capability of our condensed dataset across various deep hashing retrieval methods, we leverage

the condensed data generated by the Deep Hashing Distillation (DHD [20]) framework to train alternative deep hashing retrieval models. Specifically, we employ our method (IEM) to distill CIFAR10, generating datasets containing 10 and 50 images per class under the DHD [20] framework. These synthetic datasets are then employed to train additional deep hashing retrieval methods, namely DPN [12] and OrthHash [16].

As demonstrated in Table 5, the synthetic sets generated by IEM exhibit favorable performance on DPN [12] and OrthHash [16], effectively maintaining the original effectiveness with datasets containing 10 images per class, and achieving performance scores of 53.48% and 53.88% with datasets containing 50 images per class, respectively. The observed decrease of nearly 4% in mean average precision (mAP) when using 50 images per class can potentially be attributed to differences in retrieval abilities and early-stage augmented models among various deep hashing methods. Notably, the performance of IDC [23] on cross hashing methods is comparatively weaker than that of the original Deep Hashing Distillation (DHD [20]) dataset. In particular, IDC [23] experiences a decrease in performance of 9% and 8% with datasets containing 50 images per class, exhibiting a performance level comparable to the random selection method. These phenomena underscore the superior generalization capacity of our condensed data generated by our method, which can effectively be applied to different deep hashing methods.

img/cls		DHD	DPN	Orthhash
10	Random	23.54	25.60	25.43
	IDC	40.32	38.95	38.78
	IEM	45.85	45.75	44.54
50	Random	38.82	37.36	35.77
	IDC	47.14	38.83	39.66
	IEM	57.49	53.48	53.88

Table 5: The performance of synthetic data across deep hashing methods on CIFAR10 (50 images per class). The synthetic datasets generated by IDC [23] and IEM under DHD are trained on DPN and OrthoHash respectively.

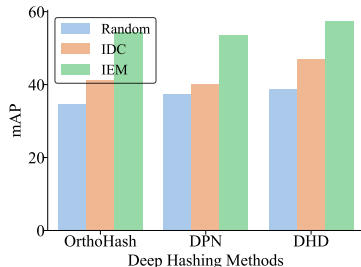


Figure 7: The performance of our method (IEM) and IDC [23] across deep hashing methods on CIFAR10 (50 images per class).

Generalization on Cross Deep Hashing Methods. In an endeavor to assess the wide-ranging applicability of our methodology across diverse deep hash retrieval models, we juxtapose the performance of our method with that of IDC [23] under a variety of deep hash models, with the findings displayed in Figure 7. IDC [23] and our method (IEM) are employed to distill CIFAR10 (50 images per class) on OrthoHash, DPN, and DHD respectively. As depicted in Figure 7, our method delivers superior performance on all three deep hashing retrieval models, exceeding random selection by an estimated 20% and IDC [23] by nearly 15%. This underscores the broad-spectrum applicability of our approach across various deep hashing retrieval methodologies. Furthermore, the deployment of IDC [23] necessitates the substitution of different gradient-matching types in accordance with the specific requirements of varying image hashing methods, a process that can be cumbersome in practical terms.

4 Conclusion

In conclusion, this paper presents IEM (Information-intensive Feature-Embedding Matching), a novel approach that represents the first endeavor in distilling datasets for deep hashing retrieval. Diverging from previous approaches in the realm of DD, our proposed technique effectively sidesteps the requirement for bi-level optimization by capitalizing on feature-embedding matching, in conjunction with the integration of multi-formation [23] and early-stage augmented models [57]. These advancements result in improved performance coupled with heightened efficiency. Notably, our method exhibits a remarkable speed advantage, being 18 times faster than the current state-of-the-art method when learning a synthetic set of 50 images per class on CIFAR10 during each distillation step. Moreover, empirical findings validate the capacity of our method to produce synthetic data characterized by high generalization ability across various network architectures and diverse image hashing retrieval methods. Notably, our technique also seamlessly adapts to prevailing image hashing retrieval frameworks, effectively bolstering the efficiency of real-world hashing retrieval.

References

- [1] Bowen Baker, Otkrist Gupta, Ramesh Raskar, and Nikhil Naik. Accelerating neural architecture search using performance prediction. *arXiv preprint arXiv:1705.10823*, 2017.
- [2] Ondrej Bohdal, Yongxin Yang, and Timothy Hospedales. Flexible dataset distillation: Learn labels instead of images. *arXiv preprint arXiv:2006.08572*, 2020.
- [3] Riccardo Cantini, Fabrizio Marozzo, Giovanni Bruno, and Paolo Trunfio. Learning sentence-to-hashtags semantic mapping for hashtag recommendation on microblogs. *ACM Transactions on Knowledge Discovery from Data (TKDD)*, 16(2):1–26, 2021.
- [4] Yue Cao, Mingsheng Long, Bin Liu, and Jianmin Wang. Deep cauchy hashing for hamming space retrieval. In *Proceedings of the IEEE Conference on Computer Vision and Pattern Recognition*, pages 1229–1237, 2018.
- [5] Zhangjie Cao, Mingsheng Long, Jianmin Wang, and Philip S Yu. Hashnet: Deep learning to hash by continuation. In *Proceedings of the IEEE international conference on computer vision*, pages 5608–5617, 2017.
- [6] George Cazenavette, Tongzhou Wang, Antonio Torralba, Alexei A Efros, and Jun-Yan Zhu. Dataset distillation by matching training trajectories. In *Proceedings of the IEEE/CVF Conference on Computer Vision and Pattern Recognition*, pages 4750–4759, 2022.
- [7] Moses S Charikar. Similarity estimation techniques from rounding algorithms. In *Proceedings of the thirty-fourth annual ACM symposium on Theory of computing*, pages 380–388, 2002.
- [8] Jia Deng, Alexander C Berg, and Li Fei-Fei. Hierarchical semantic indexing for large scale image retrieval. In *CVPR 2011*, pages 785–792. IEEE, 2011.
- [9] Jiawei Du, Yidi Jiang, Vincent TF Tan, Joey Tianyi Zhou, and Haizhou Li. Minimizing the accumulated trajectory error to improve dataset distillation. *arXiv preprint arXiv:2211.11004*, 2022.
- [10] Ali Mamdouh Elkahky, Yang Song, and Xiaodong He. A multi-view deep learning approach for cross domain user modeling in recommendation systems. In *Proceedings of the 24th international conference on world wide web*, pages 278–288, 2015.
- [11] Bin Fan, Dave G Andersen, Michael Kaminsky, and Michael D Mitzenmacher. Cuckoo filter: Practically better than bloom. In *Proceedings of the 10th ACM International on Conference on emerging Networking Experiments and Technologies*, pages 75–88, 2014.
- [12] Lixin Fan, Kam Woh Ng, Ce Ju, Tianyu Zhang, and Chee Seng Chan. Deep polarized network for supervised learning of accurate binary hashing codes. In *IJCAI*, pages 825–831, 2020.
- [13] David Gorisse, Matthieu Cord, and Frederic Precioso. Locality-sensitive hashing for chi2 distance. *IEEE transactions on pattern analysis and machine intelligence*, 34(2):402–409, 2011.
- [14] Amirhossein Habibian, Thomas Mensink, and Cees GM Snoek. Discovering semantic vocabularies for cross-media retrieval. In *Proceedings of the 5th ACM on International Conference on Multimedia Retrieval*, pages 131–138, 2015.
- [15] Kaiming He, Xiangyu Zhang, Shaoqing Ren, and Jian Sun. Deep residual learning for image recognition. In *Proceedings of the IEEE conference on computer vision and pattern recognition*, pages 770–778, 2016.
- [16] Jiun Tian Hoe, Kam Woh Ng, Tianyu Zhang, Chee Seng Chan, Yi-Zhe Song, and Tao Xiang. One loss for all: Deep hashing with a single cosine similarity based learning objective. *Advances in Neural Information Processing Systems*, 34:24286–24298, 2021.
- [17] Shengyuan Hu, Jack Goetz, Kshitiz Malik, Hongyuan Zhan, Zhe Liu, and Yue Liu. Fedsynth: Gradient compression via synthetic data in federated learning. *arXiv preprint arXiv:2204.01273*, 2022.

- [18] Gao Huang, Zhuang Liu, Laurens Van Der Maaten, and Kilian Q Weinberger. Densely connected convolutional networks. In *Proceedings of the IEEE conference on computer vision and pattern recognition*, pages 4700–4708, 2017.
- [19] Piotr Indyk and Ramee Motwani. Approximate nearest neighbors: towards removing the curse of dimensionality. In *Proceedings of the thirtieth annual ACM symposium on Theory of computing*, pages 604–613, 1998.
- [20] Young Kyun Jang, Geonmo Gu, ByungSoo Ko, Isaac Kang, and Nam Ik Cho. Deep hash distillation for image retrieval. *arXiv preprint arXiv:2112.08816*, 2021.
- [21] Zixuan Jiang, Jiaqi Gu, Mingjie Liu, and David Z Pan. Delving into effective gradient matching for dataset condensation. *arXiv preprint arXiv:2208.00311*, 2022.
- [22] Wei Jin, Lingxiao Zhao, Shichang Zhang, Yozen Liu, Jiliang Tang, and Neil Shah. Graph condensation for graph neural networks. *arXiv preprint arXiv:2110.07580*, 2021.
- [23] Jang-Hyun Kim, Jinuk Kim, Seong Joon Oh, Sangdoon Yun, Hwanjun Song, Joonhyun Jeong, Jung-Woo Ha, and Hyun Oh Song. Dataset condensation via efficient synthetic-data parameterization. In *International Conference on Machine Learning*, pages 11102–11118. PMLR, 2022.
- [24] Alex Krizhevsky, Geoffrey Hinton, et al. Learning multiple layers of features from tiny images. In *Proceedings of the 26th Annual Conference on Neural Information Processing Systems (NIPS)*, pages 1–9, Vancouver, BC, Canada, 2009.
- [25] Alex Krizhevsky, Ilya Sutskever, and Geoffrey E Hinton. Imagenet classification with deep convolutional neural networks. *Communications of the ACM*, 60(6):84–90, 2017.
- [26] Brian Kulis and Kristen Grauman. Kernelized locality-sensitive hashing. *IEEE Transactions on Pattern Analysis and Machine Intelligence*, 34(6):1092–1104, 2011.
- [27] Yann LeCun, Yoshua Bengio, and Geoffrey Hinton. Deep learning. *nature*, 521(7553):436–444, 2015.
- [28] Guang Li, Ren Togo, Takahiro Ogawa, and Miki Haseyama. Soft-label anonymous gastric x-ray image distillation. In *2020 IEEE International Conference on Image Processing (ICIP)*, pages 305–309. IEEE, 2020.
- [29] Guang Li, Ren Togo, Takahiro Ogawa, and Miki Haseyama. Compressed gastric image generation based on soft-label dataset distillation for medical data sharing. *Computer Methods and Programs in Biomedicine*, 227:107189, 2022.
- [30] Ping Li, Arnd Konig, and Wenhao Gui. b-bit minwise hashing for estimating three-way similarities. *Advances in Neural Information Processing Systems*, 23, 2010.
- [31] Qi Li, Zhenan Sun, Ran He, and Tieniu Tan. Deep supervised discrete hashing. *Advances in neural information processing systems*, 30, 2017.
- [32] Kevin Lin, Huei-Fang Yang, Jen-Hao Hsiao, and Chu-Song Chen. Deep learning of binary hash codes for fast image retrieval. In *Proceedings of the IEEE conference on computer vision and pattern recognition workshops*, pages 27–35, 2015.
- [33] Mengyang Liu, Shanchuan Li, Xinshi Chen, and Le Song. Graph condensation via receptive field distribution matching. *arXiv preprint arXiv:2206.13697*, 2022.
- [34] Wojciech Masarczyk and Ivona Tautkute. Reducing catastrophic forgetting with learning on synthetic data. In *Proceedings of the IEEE/CVF Conference on Computer Vision and Pattern Recognition Workshops*, pages 252–253, 2020.
- [35] Timothy Nguyen, Zhourong Chen, and Jaehoon Lee. Dataset meta-learning from kernel ridge-regression. *arXiv preprint arXiv:2011.00050*, 2020.

- [36] Timothy Nguyen, Roman Novak, Lechao Xiao, and Jaehoon Lee. Dataset distillation with infinitely wide convolutional networks. *Advances in Neural Information Processing Systems*, 34:5186–5198, 2021.
- [37] Prashant Pandey, Michael A Bender, Rob Johnson, and Rob Patro. A general-purpose counting filter: Making every bit count. In *Proceedings of the 2017 ACM international conference on Management of Data*, pages 775–787, 2017.
- [38] Matthew Riley, Eric Heinen, and Joydeep Ghosh. A text retrieval approach to content-based audio retrieval. In *Int. Symp. on Music Information Retrieval (ISMIR)*, pages 295–300, 2008.
- [39] Olga Russakovsky, Jia Deng, Hao Su, Jonathan Krause, Sanjeev Satheesh, Sean Ma, Zhiheng Huang, Andrej Karpathy, Aditya Khosla, Michael Bernstein, et al. Imagenet large scale visual recognition challenge. *International journal of computer vision*, 115:211–252, 2015.
- [40] Levent Sagun, Utku Evci, V Ugur Guney, Yann Dauphin, and Leon Bottou. Empirical analysis of the hessian of over-parametrized neural networks. *arXiv preprint arXiv:1706.04454*, 2017.
- [41] Mattia Sangermano, Antonio Carta, Andrea Cossu, and Davide Bacciu. Sample condensation in online continual learning. In *2022 International Joint Conference on Neural Networks (IJCNN)*, pages 01–08. IEEE, 2022.
- [42] Seungjae Shin, Heesun Bae, Donghyeok Shin, Weonyoung Joo, and Il-Chul Moon. Loss-curvature matching for dataset selection and condensation. In *International Conference on Artificial Intelligence and Statistics*, pages 8606–8628. PMLR, 2023.
- [43] Jingkuan Song, Yi Yang, Zi Huang, Heng Tao Shen, and Richang Hong. Multiple feature hashing for real-time large scale near-duplicate video retrieval. In *Proceedings of the 19th ACM international conference on Multimedia*, pages 423–432, 2011.
- [44] Rui Song, Dai Liu, Dave Zhenyu Chen, Andreas Festag, Carsten Trinitis, Martin Schulz, and Alois Knoll. Federated learning via decentralized dataset distillation in resource-constrained edge environments. *arXiv preprint arXiv:2208.11311*, 2022.
- [45] Benno Stein. Principles of hash-based text retrieval. In *Proceedings of the 30th annual international ACM SIGIR conference on Research and development in information retrieval*, pages 527–534, 2007.
- [46] Shupeng Su, Zhisheng Zhong, and Chao Zhang. Deep joint-semantics reconstructing hashing for large-scale unsupervised cross-modal retrieval. In *Proceedings of the IEEE/CVF international conference on computer vision*, pages 3027–3035, 2019.
- [47] Iliia Sucholutsky and Matthias Schonlau. Soft-label dataset distillation and text dataset distillation. In *2021 International Joint Conference on Neural Networks (IJCNN)*, pages 1–8. IEEE, 2021.
- [48] Mir Saman Tajbakhsh and Jamshid Bagherzadeh. Microblogging hash tag recommendation system based on semantic tf-idf: Twitter use case. In *2016 IEEE 4th International Conference on Future Internet of Things and Cloud Workshops (FiCloudW)*, pages 252–257. IEEE, 2016.
- [49] Jingdong Wang, Ting Zhang, Nicu Sebe, Heng Tao Shen, et al. A survey on learning to hash. *IEEE transactions on pattern analysis and machine intelligence*, 40(4):769–790, 2017.
- [50] Jun Wang, Sanjiv Kumar, and Shih-Fu Chang. Semi-supervised hashing for scalable image retrieval. In *2010 IEEE Computer Society Conference on Computer Vision and Pattern Recognition*, pages 3424–3431. IEEE, 2010.
- [51] Kai Wang, Bo Zhao, Xiangyu Peng, Zheng Zhu, Shuo Yang, Shuo Wang, Guan Huang, Hakan Bilen, Xinchao Wang, and Yang You. Cafe: Learning to condense dataset by aligning features. In *Proceedings of the IEEE/CVF Conference on Computer Vision and Pattern Recognition*, pages 12196–12205, 2022.
- [52] Tongzhou Wang, Jun-Yan Zhu, Antonio Torralba, and Alexei A Efros. Dataset distillation. *arXiv preprint arXiv:1811.10959*, 2018.

- [53] Gengshen Wu, Jungong Han, Yuchen Guo, Li Liu, Guiguang Ding, Qiang Ni, and Ling Shao. Unsupervised deep video hashing via balanced code for large-scale video retrieval. *IEEE Transactions on Image Processing*, 28(4):1993–2007, 2018.
- [54] Rongkai Xia, Yan Pan, Hanjiang Lai, Cong Liu, and Shuicheng Yan. Supervised hashing for image retrieval via image representation learning. In *Proceedings of the AAAI conference on artificial intelligence*, 2014.
- [55] Chenggang Yan, Biao Gong, Yuxuan Wei, and Yue Gao. Deep multi-view enhancement hashing for image retrieval. *IEEE Transactions on Pattern Analysis and Machine Intelligence*, 43(4):1445–1451, 2020.
- [56] Li Yuan, Tao Wang, Xiaopeng Zhang, Francis EH Tay, Zequn Jie, Wei Liu, and Jiashi Feng. Central similarity quantization for efficient image and video retrieval. In *Proceedings of the IEEE/CVF conference on computer vision and pattern recognition*, pages 3083–3092, 2020.
- [57] Lei Zhang, Jie Zhang, Bowen Lei, Subhabrata Mukherjee, Xiang Pan, Bo Zhao, Caiwen Ding, Yao Li, and Dongkuan Xu. Accelerating dataset distillation via model augmentation. *arXiv preprint arXiv:2212.06152*, 2022.
- [58] Bo Zhao and Hakan Bilen. Dataset condensation with differentiable siamese augmentation. In *International Conference on Machine Learning*, pages 12674–12685. PMLR, 2021.
- [59] Bo Zhao and Hakan Bilen. Dataset condensation with distribution matching. In *Proceedings of the IEEE/CVF Winter Conference on Applications of Computer Vision*, pages 6514–6523, 2023.
- [60] Bo Zhao, Konda Reddy Mopuri, and Hakan Bilen. Dataset condensation with gradient matching. *arXiv preprint arXiv:2006.05929*, 2020.
- [61] Han Zhu, Mingsheng Long, Jianmin Wang, and Yue Cao. Deep hashing network for efficient similarity retrieval. In *Proceedings of the AAAI conference on Artificial Intelligence*, 2016.

This comes as the supplementary material to the paper *Towards Efficient Deep Hashing Retrieval: Condensing Your Data via Feature-Embedding Matching*. The appendix is structured as follows:

A. Related works and Preliminaries. We first take a brief introduction of the DD and deep hashing retrieval, and show a detailed description of gradient-matching methods and distribution-matching method.

B. Implementation details of experiments. We show more details of our experiments.

C. Additional experiments.

A Related works and Preliminaries

A.1 Related Works

Deep Hashing Image Retrieval. Image retrieval based on hashing has emerged as an efficient methodology to address the computational challenges associated with handling high-dimensional and large-scale datasets. An expanding body of research has introduced numerous approaches that extend traditional deep hashing algorithms, CNNH [54] employs a network that establishes paired connections between CNN labels to generate compact hash codes. DHN [61] generates hash codes by approximating discrete values through relaxation techniques. HashNet [5] assesses the similarity between hash codes and addresses challenges related to data imbalance. DCH [4] reduces the Hamming distance of hash codes belonging to the same target. Except for the conventional ways, The methodologies that revolve around identifying hash centers have yielded promising outcomes in recent studies. CSQ [56] introduces binary hash centers, ensuring that the hash codes align with their respective hash representatives. OrthoHash [16] proposes a novel deep hashing model with a single learning objective. Furthermore, DHD [20] pioneers a self-distilled strategy to mitigate the discrepancy arising from image augmentation, with the additional updating of the proposed hash proxies to enhance the global similarity of the hash codes. In this paper, we utilize DHD [20], the state-of-the-art deep hashing retrieval method, as the retrieval benchmark for dataset distillation. While our primary emphasis lies on investigating the distillation method within deep supervised hashing methods, it is important to acknowledge the inclusion of other methodologies in the survey [49].

Dataset Distillation. The pioneering investigation carried out by [52] involves the utilization of gradient-based hyper parameter optimization for learning purposes,generating synthesis of small-scale training data under the constraints imposed by limited storage resources. Expanding on this foundation, several approaches have been proposed, including the optimization of soft labels and data [2, 47], data optimization through the utilization of the neural tangent kernel [35, 36], distribution matching in the feature-embedding space [51, 59], Training Trajectory matching [6, 9], gradient-pair matching [21, 58, 60], data space enlargement and regularization for synthetic data optimization [23], and efficiency enhancement via Model Augmentation [57]. Dataset distillation has been studied across various domains, including continual learning [34, 41], network architecture search [1, 60], federated learning [17, 44], graph neural networks [22, 33], and medical computing [28, 29]. Apart from the concerted efforts made towards optimizing performance and broadening the domain of applications, scant scholarly attention has been paid to the systematic construction of datasets intended to enable effective deep hash retrieval. This embodies a pivotal and practical challenge that bears close relevance to the real-world utility of DD.

A.2 Detailed DD

DD with Gradient Matching. Gradient-matching method [23, 58, 60] matches the training trajectories by minimize the gradients distance between synthetic data S and real data T . The general optimization objection can be defined as:

$$L = \sum_{c=0}^{C-1} D(\nabla_{\theta_t} L(\mathcal{X}^c; \theta_t), \nabla_{\theta_t} L(S^c; \theta_t)), \quad (1)$$

where c denotes number of training class, $D(,)$ denotes gradient distance between the synthetic and original dataset, $L(,)$ denotes the cross-entropy loss function. ∇ denotes the average loss gradient with respect to a model θ_t .

DD with Distribution Matching. The distillation method of distribution-matching matches the distributions between synthetic and real dataset in feature space. DM extracts embedded features from the real and condensed sets using a feature extractor ψ_v , and then employs the empirical estimation of the maximum mean discrepancy (MMD) to minimize the discrepancy between the feature distributions. The synthetic sets are optimized by the function below:

$$\mathcal{L}(\mathcal{S}) = \sum_{c=1}^C \|\psi_v(\mathcal{B}_S^c) - \psi_v(\mathcal{B}_T^c)\|^2, \quad (2)$$

where c denotes number of training class, \mathcal{B}_S^c and \mathcal{B}_T^c represent the batch samples of the corresponding c -th class. Although distribution-matching method avoids the expensive bi-level optimization process, needing less memory requirement and training time, it underperforms the gradient-matching methods generally [23, 58, 60].

B Implementation details of experiments

B.1 Datasets in detail

In this paper, training sets of CIFAR10 and ImageNet-subset are different from previous works [23, 58, 59] due to retrieval tasks. The details are in Table 6.

Table 6: Description of the image retrieval datasets.

Dataset	Database	Training images	Querying images	category
CIFAR10	59000	5000	1000	10
ImageNet10	13000	1300	500	10
ImageNet20	26000	2600	1000	20

B.2 Experimental Settings.

Given the distinctive objective of the present approach compared to previous DD techniques [23, 58, 59], certain modifications have been implemented to cater to the specific requirements of image hashing retrieval. Specifically, in the gradient-matching dataset distillation method (DSA [58] and IDC [23]), gradients are perplexing and challenging in the context of image hashing retrieval. We select DHD [20] (the-state-of-art) as our image hashing baseline. DHD [20] addresses the discrepancy between real and Hamming space provoked by data augmentation in deep hashing by \mathcal{L}_{SDH} , learns global discriminative hash codes by ℓ_{HP} and reduces the quantization error by ℓ_{bce-Q} .

For IDC [23] and DSA [58], in order to generate synthetic set effectively and fairly, we compute all gradients generated by DHD [20] and perform gradients-matching between real and synthetic sets. The details are in the Algorithm 2. The inner loops, factors, augmentation strategy, and other hyper-parameters remain consistent with those employed in IDC [23] and DSA [58]. As DM [59] solely involves the distribution matching in feature space, we maintain alignment in the distillation steps with DM [59]. Our method is built upon the framework of IDC [23].

For our method (IEM), We run all experiments of CIFAR10 on RTX-2080 Ti and ImageNet-subset on RTX-3090. In our experiments, we set the inner iterations $M = 300$ for CIFAR10, 200 for ImageNet-subset. For CIFAR10, the data learning rate $\lambda = 0.005$, the network training (DHD [20]) on synthetic data is performed using the Adam optimizer with the learning rate of 0.03 and weight-decay of value 0.000006. For ImageNet10, the data learning rate $\lambda = 10$, and $\lambda = 20$ for ImageNet20. The network training (DHD [20]) on synthetic data is performed using the Adam optimizer with the learning rate of 0.004 and weight-decay of value 0.000006. The training details are in Algorithm (See page 4 in the main paper).

Algorithm 2: Information-Intensive Dataset Condensation for DHD [20]

Input: Training set \mathcal{T} **Output:** Synthetic set \mathcal{S} **Notation:** Multi-formation function f , parameterized augmentation function a_ω , mixup function h , loss function l , number of classes N_c , loss function \mathcal{L}_{SDH} , ℓ_{bce-Q} and ℓ_{HP} , parameters θ of DHD consists: $\theta_E, \theta_H, \theta_P$ **Definition:**

$$D_1(B, B'; \theta_{E,H}) = \|\nabla_{\theta_{E,H}} \ell_{(SDH+bce-Q)}(\theta_{E,H}; B) - \nabla_{\theta_{E,H}} \ell_{(SDH+bce-Q)}(\theta_{E,H}; B')\|$$

$$D_2(B, B'; \theta_P) = \|\nabla_{\theta_P} \ell_{HP}(\theta_P; B) - \nabla_{\theta_P} \ell_{HP}(\theta_P; B')\|$$

repeat Initialize or load pretrained network θ_1 **for** $i = 1$ **to** M **do** **for** $c = 1$ **to** N_c **do** Sample an intra-class mini-batch $T_c \sim \mathcal{T}, S_c \sim \mathcal{S}$

Update:

$$S_c \leftarrow S_c - \lambda \nabla_{S_c} (D_1(a_\omega(f(S_c)), a_\omega(T_c); \theta_{E,H}) + D_2(a_\omega(f(S_c)), a_\omega(T_c); \theta_P))$$

end Sample a mini-batch $T \sim \mathcal{T}$ Update $\theta_{i+1} \leftarrow \theta_i - \eta \nabla_{\theta} \ell(\theta_i; h(a_{\omega'}(T)))$ **end****until** convergence;

C Additional Experiments

C.1 More efficiency results on Datasets

CIFAR10. As shown in Table 7, our method surpasses the state-of-art IDC [23] 1%, 5%, 11% on 1/10/50 image(s) per class. We also conduct a comparative analysis of the IDC [23] and our method, evaluating their respective performances at convergence time ratios of 1/5 and 1/10. The results reveal that our method exhibits superior performance within a shorter temporal context. Notably, our method achieves 39.65% in a mere 3 minutes when distilling 10 images per class, rivaling the best performance of IDC [23]. Furthermore, a remarkable mAP of 53.25% is achieved within a time frame of only 6 minutes when distilling 50 images per class, significantly surpassing the effectiveness of IDC [23]. These findings substantiate the concurrent consideration of efficiency and efficacy in our method, obviating the necessity for protracted training and computational expenses while surpassing prevailing DD methods.

ImageNet. We study the performances on high-resolution ImageNet10/20 dataset using previous DD methods [23, 58, 59] and our method. Our method demonstrates performance comparable to IDC [23], but showcasing enhanced effectiveness within constrained temporal conditions. Table 7 corroborates the superiority of our approach under 5× and 10× speed ups, surpassing IDC’s [23] performance while necessitating reduced time expenditure. Figure 9a and Figure 9b illustrate that when distilling ImageNet-subset to 1 image per class, our method achieves a level of precision comparable to IDC [23]. However, the noteworthy aspect of our method lies in its rapid convergence. The visual representation in the Figure 9c clearly indicates that our method requires a lower training cost while maintaining a satisfactory performance. These findings serve as empirical evidence attesting to the efficacy of our method on high-resolution dataset, manifesting performance equivalence to prevailing superior methods while circumventing substantial training expenses.

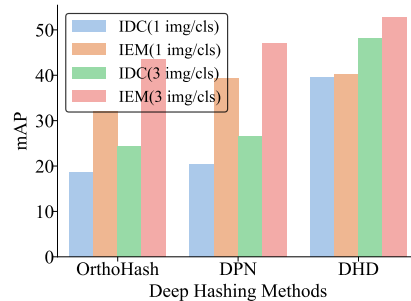


Figure 8: The performance of our method (IEM) and IDC [23] across deep hashing methods on ImageNet10 (1/3image(s) per class). img(s)/cls represents the number of image(s) per class

	Imgs/Ratio	Random	DM	DSA	IDC1	IEM1	IDC5	IEM5	IDC10	IEM10
CIFAR10	1/0.2	15.35	18.62	15.73	24.65	25.82	25.02(28min)	23.62(13min)	24.78(97.8min)	22.88(6min)
	10/2%	23.54	30.23	28.32	40.32	45.85	36.22(90min)	39.65(3min)	35.57(45min)	37.13(1min)
	50/10%	38.82	43.43	40.58	46.21	57.49	47.04(18min)	54.60(19.5min)	-	53.25(6min)
ImageNet10	1/0.77%	17.62	20.43	18.42	39.55	40.32	35.06(0.93h)	34.04(0.47h)	33.54(0.4h)	33.63(0.24h)
	3/2.3%	21.22	24.10	21.78	48.14	52.79	44.34(0.47h)	49.98(0.4h)	44.18(0.23h)	48.35(0.15h)
ImageNet20	1/0.77%	10.14	11.22	10.84	26.60	25.70	22.67(1.75h)	23.68(0.82h)	22.97(1.5h)	22.53(0.41h)
	3/2.3%	10.71	12.96	11.78	34.48	35.12	32.42(0.9h)	33.31(0.4h)	32.29(0.45h)	33.25(0.13h)

Table 7: Comparing to different training set synthesis methods on deep hashing retrieval on CIFAR10 and ImageNet-subset. The terms Imgs/Ratio denote the number of image(s) per class and the condensed set size as a percentage of the entire training set size. We compare the same acceleration levels between IDC [23] and our method on 5 \times , 10 \times .

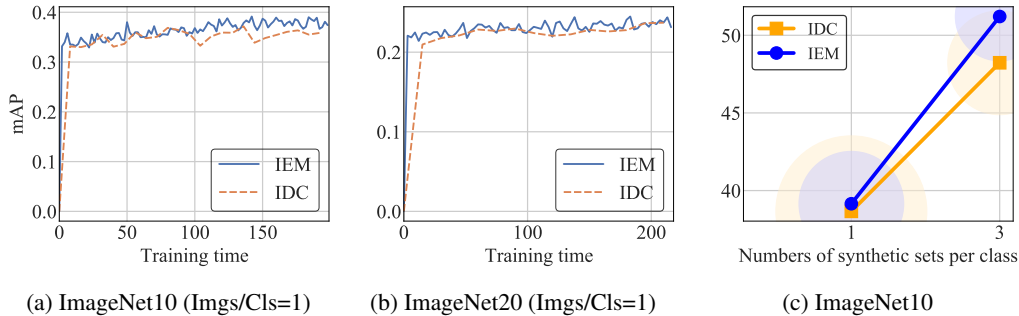


Figure 9: Performance comparison across training time of IEM and IDC [23]. The utilization of blue and green circles in Figure 6f signifies the temporal requirements for achieving convergence in IEM and IDC [23], respectively. The dimensions of the circles represent the corresponding time duration needed for convergence in each method.

C.2 Generalization on Cross Deep Hashing Methods.

To evaluate the generalization ability of our approach across different hashing retrieval methods, we employ two distinct methods, namely DPN [12] and OrthoHash [16], for condensing the high-resolution ImageNet10 dataset, which is condensed to 1 and 3 image(s) per class, respectively, as illustrated in the provided figure 8. Our results indicate that, when applied to high-resolution datasets, our approach significantly outperforms the IDC [23] across different deep hashing retrieval methods. Conversely, IDC [23] exhibits inferior compression outcomes when applied to both DPN [12] and OrthoHash [16] approaches, which suggests that IDC [23] is constrained by specific deep hashing retrieval models. These results show that our method effectively adapt to prevailing deep hashing retrieval methods, circumventing the computational costs arising from laborious and protracted gradient comparisons, enabling it to achieve stable and superior distillation performance in reality.